APPLIED AND ENVIRONMENTAL MICROBIOLOGY, Aug. 2006, p. 5173–5180 Vol. 72, No. 8
0099-2240/06/$08.00+0 doi:10.1128/AEM.00568-06

Resolution of Distinct Membrane-Bound Enzymes from *Enterobacter cloacae* SLD1a-1 That Are Responsible for Selective Reduction of Nitrate and Selenate Oxyanions

Helen Ridley,[1] Carys A. Watts,[1] David J. Richardson,[2] and Clive S. Butler[1]*

Institute for Cell and Molecular Biosciences, University of Newcastle, Newcastle upon Tyne NE2 4HH, United Kingdom,[1] *and School of Biological Sciences, University of East Anglia, Norwich NR4 7TJ, United Kingdom*[2]

Received 9 March 2006/Accepted 15 May 2006

Enterobacter cloacae **SLD1a-1 is capable of reductive detoxification of selenate to elemental selenium under aerobic growth conditions. The initial reductive step is the two-electron reduction of selenate to selenite and is catalyzed by a molybdenum-dependent enzyme demonstrated previously to be located in the cytoplasmic membrane, with its active site facing the periplasmic compartment (C. A. Watts, H. Ridley, K. L. Condie, J. T. Leaver, D. J. Richardson, and C. S. Butler, FEMS Microbiol. Lett. 228:273–279, 2003). This study describes the purification of two distinct membrane-bound enzymes that reduce either nitrate or selenate oxyanions. The nitrate reductase is typical of the NAR-type family, with α and β subunits of 140 kDa and 58 kDa, respectively. It is expressed predominantly under anaerobic conditions in the presence of nitrate, and while it readily reduces chlorate, it displays no selenate reductase activity in vitro. The selenate reductase is expressed under aerobic conditions and expressed poorly during anaerobic growth on nitrate. The enzyme is a heterotrimeric (αβγ) complex with an apparent molecular mass of ~600 kDa. The individual subunit sizes are ~100 kDa (α), ~55 kDa (β), and ~36 kDa (γ), with a predicted overall subunit composition of $\alpha_3\beta_3\gamma_3$. The selenate reductase contains molybdenum, heme, and nonheme iron as prosthetic constituents. Electronic absorption spectroscopy reveals the presence of a *b*-type cytochrome in the active complex. The apparent K_m for selenate was determined to be ~2 mM, with an observed V_{max} of 500 nmol SeO_4^{2-} min^{-1} mg^{-1} (k_{cat}, ~5.0 s^{-1}). The enzyme also displays activity towards chlorate and bromate but has no nitrate reductase activity. These studies report the first purification and characterization of a membrane-bound selenate reductase.**

Selenium (Se) is a naturally occurring trace element (12). It is essential for humans and animals (27), but in its most oxidized form, selenate (SeO_4^{2-}), it is highly soluble and can present a significant hazard to health and the environment (12, 24). Naturally high levels of selenate are found in America and Canada, where, for example, Se-contaminated drainage water from the seleniferous rich soils of California's San Joaquin Valley has been a major cause of death and deformities in waterfowl and other wildlife. However, it is more common that the human activities of petroleum refining, mining, fossil fuel combustion, and the use of selenium-rich fertilizers and feed stocks in agriculture contribute significantly to generating selenate-contaminated environments (12). Most of the selenium discharge in waste/runoff water exists as the soluble oxyanion selenate (SeO_4^{2-}), with lesser amounts of selenite (SeO_3^{2-}). These soluble oxyanions are the primary forms of selenium in aerated environments. The transformation of selenate to selenite in nature occurs primarily by microbial processes (28), and selenate does not readily undergo chemical reduction under ambient pH and temperature conditions.

One of the most successful methods for selenate detoxification is via biotic reduction of selenate to selenite (SeO_3^{2-}) catalyzed by a microbial reductase, followed by either biotic or abiotic reduction of selenite to insoluble, less toxic elemental selenium (Se^0) (16, 28). Microbes that can reduce the selenium oxyanions selenate (SeO_4^{2-}) and selenite (SeO_3^{2-}) are not restricted to any particular group/subgroup of prokaryotes, and examples are found throughout the bacterial and archaeal domains (18, 22, 23, 28). It has been suggested that selenate reduction may be catalyzed in many cases by a secondary reaction of the bacterial nitrate reductases, and a selenate reductase activity of both the membrane-bound (NAR) and periplasmic (NAP) nitrate reductases from *Ralstonia eutropha*, *Paracoccus denitrificans*, and *Paracoccus pantotrophus* has been reported (5, 25). Similarly, both NarG and NarZ in membrane fractions from *Escherichia coli* have been reported to show selenate reductase activity, but only when assayed in the presence of excess (160 mM) sodium selenate (1). Clearly, it is evident that membrane-bound nitrate reductases are poor reducers of selenate (1, 31) and may not contribute significantly to global selenate reduction, particularly in areas enriched with both selenate and nitrate. Consequently, novel enzyme systems that selectively catalyze the reduction of selenate have been sought (2, 26, 32), and to date, detailed biochemical studies have been limited mainly to a single species, *Thauera selenatis* (7, 17, 19, 26). Under anaerobic conditions, *T. selenatis* can respire with selenate as the sole terminal electron acceptor. The selenate reductase (SER) from *T. selenatis* is a periplasmic trimeric enzyme with an apparent molecular mass of ~180 kDa (26). The three subunits consist of SerA (96 kDa), SerB (40 kDa), and SerC (23 kDa). The SerA subunit has an N-terminal cysteine-rich motif, probably coordinating a [4Fe-4S] cluster, and also contains the molybdenum (Mo) active site in

* Corresponding author. Mailing address: Institute for Cell and Molecular Biosciences, University of Newcastle, Newcastle upon Tyne NE2 4HH, United Kingdom. Phone: 44 (191) 222 8800. Fax: 44 (191) 222 7424. E-mail: c.s.butler@ncl.ac.uk.

the form of the molybdopterin guanine dinucleotide (*bis*-MGD) cofactor (20, 26). The SerB subunit also has a number of cysteine-rich motifs, which again suggest the presence of iron-sulfur clusters. The SerC subunit contains a *b*-type cytochrome, as shown by visible absorption spectroscopy (26). DNA sequence analysis of *T. selenatis* has identified the presence of a fourth component (SerD) that may function as a specific chaperone assembly protein involved in MGD cofactor insertion into SerA (17). A membrane-bound component analogous to NapC or NarI in the nitrate reductase systems has not yet been identified, so the process by which SerABC receives electrons from the quinol pool remains to be established. The selenate reductase shows surprising substrate selectivity and does not reduce nitrate or sulfate (26). Amino acid sequence alignment of SerA with the periplasmic (NapA) and membrane-bound (NarG) nitrate reductases from all available sequences has shown that SerA is more closely related to NarG than NapA, despite its periplasmic location. The highly conserved Asp^{222} residue (*E. coli* NarG numbering), shown to coordinate the Mo in recent NAR X-ray structures (4, 14), is also present in SerA, placing SerA as a member of a distinct subgroup of the D-group (type II) molybdo-enzymes, which also include chlorate reductase (ClrA) from *Ideonella dechloratans* (30), dimethyl sulfide dehydrogenase (DdhA) from *Rhodovulum sulfidophilum* (21), perchlorate reductase (PcrA) from *Dechloromonas* sp. (3), and ethylbenzene dehydrogenase (EbdA) from *Azoarcus* sp.-like strain EbN1 (13).

Enterobacter cloacae SLD1a-1 (ATCC 700258), a bacterium isolated from Se-contaminated drainage water in the San Joaquin Valley, California, can also reduce Se oxyanions to elemental selenium (9, 18, 31, 32) but cannot utilize selenate as the sole electron acceptor when grown anaerobically on nonfermentable carbon sources (32). However, it is the ability of this organism to readily catalyze the reduction of selenate to selenium under aerobic conditions that has interested those developing bioremediation strategies. The observation that elemental selenium accumulates near the cytoplasmic membrane prior to expulsion has led to the suggestion that the reduction of selenate to selenite by *E. cloacae* SLD1a-1 may occur via a membrane-bound selenate reductase expressed under aerobic conditions (18). We have suggested previously that *E. cloacae* SLD1a-1 expresses two distinct membrane-bound reductases for the reduction of nitrate and selenate and presented evidence that the selenate reductase is a molybdo-enzyme associated with the cytoplasmic membrane and orientated such that its active site faces the periplasmic compartment (32). For the present study, we have purified and characterized both the respiratory membrane-bound nitrate reductase and the membrane-bound selenate reductase from *E. cloacae* SLD1a-1. The subunit composition, cofactor analysis, and substrate selectivity of each enzyme are presented.

MATERIALS AND METHODS

Growth of *E. cloacae* SLD1a-1 and preparation of cell extracts. *E. cloacae* SLD1a-1 was purchased from the American Type Culture Collection (ATCC 700258) and grown under both aerobic and anaerobic conditions. The constitutive expression of selenate reductase meant that selenate was not required in the growth medium, and no nitrate was supplemented because it is known to prevent the reduction to elemental selenium. When cells were grown aerobically, a preculture was prepared by inoculating a glycerol stock (500 μl) into Luria-Bertani (LB) medium (200 ml) and incubating it in an orbital incubator overnight at 37°C and 180 rpm. A New Brunswick Bioflow 110 fermentor containing LB medium (10 liters) supplemented with sodium molybdate (1 mM) was equilibrated to 37°C and purged with a constant filtered airflow (10 liters/min). The preculture (120 ml) was inoculated into the medium to an optical density at 600 nm of 0.1 and grown at 37°C with agitation at 300 rpm for 2 h. The agitation rate was then increased to 400 rpm, and the culture was grown for another hour at 37°C. When grown under anaerobic conditions, cells were again cultured in the 10-liter fermentor in BSM medium (10, 17, 32) supplemented with glycerol and formate (15 mM) as the sole sources of carbon and electrons and with nitrate (10 mM) as the sole electron acceptor. The growth medium was purged with O_2-free nitrogen gas for 1 h prior to inoculation, and no air supply was provided during growth. Cells were harvested by centrifugation at 6,000 rpm (Beckman JA10 rotor) at 4°C for 15 min and then stored on ice. Cell pellets were resuspended in 50 mM Tris buffer, pH 8.6 (in two 50-ml suspensions). Each 50-ml suspension was sonicated at an amplitude setting of 14 microns for 15 min (20 seconds on/off pulsing). A protease inhibitor cocktail (Sigma P8465) and AEBSF [4-(2-aminoethyl)benzenesulfonyl fluoride] (100 μg/ml) were added, and the unbroken cell fraction was removed by centrifugation at 6,000 rpm at 4°C for 30 min. The membrane fraction was collected by ultracentrifugation at 45,000 rpm at 4°C for 60 min and homogenized in 50 mM Tris buffer, pH 8.6. Activity assays were performed, and the membrane fraction was stored at 4°C or −20°C prior to purification. Membrane proteins were solubilized by treatment with either 2.5% (wt/vol) octyl β-D-glucopyranoside (OGP) or nonaethylene glycol monododecyl ether (Thesit) for 90 min at room temperature, with constant agitation. The solubilized membrane fraction was collected as the supernatant after ultracentrifugation at 45,000 rpm (Beckman 70 Ti rotor) at 4°C for 90 min. The protein concentration was determined using the Bio-Rad protein assay following the manufacturer's instructions.

Purification of nitrate and selenate reductases from *E. cloacae* SLD1a-1 membranes. The nitrate reductase was purified from solubilized membranes extracted from anaerobically grown cells by a two-step anion-exchange chromatography protocol. A Source 30Q column was equilibrated with 50 mM Tris-HCl, 2% (wt/vol) OGP, pH 8.6 (buffer A), on an AKTA Prime (Amersham Biosciences) purification system using a constant flow rate of 1 ml/min. The solubilized membrane fraction (10 ml) was filtered through a 0.2-μm filter and loaded onto the column at 1 ml/min, and the flowthrough was collected. The column was washed with 100% buffer A at 1 ml/min until all unbound proteins were removed. The bound proteins were eluted using a step gradient of 20% 50 mM Tris-HCl, 1 M NaCl, 2% (wt/vol) OGP, pH 8.6 (buffer B), and the proteins were collected in 0.5-ml fractions. A large protein peak was eluted at 200 mM NaCl, with the nitrate reductase activity located to the right of the peak. The active fractions were pooled and desalted using two 5-ml desalting columns (Amersham Biosciences) in series on an AKTA Prime system. The pooled fractions were concentrated, loaded onto a Resource 15Q column, equilibrated with buffer A, and eluted using a 0 to 100% gradient of buffer B. The maximum peak with nitrate reductase activity was eluted at 290 mM NaCl. Active fractions were pooled, spin concentrated, and frozen at −20°C prior to use.

The selenate reductase was purified from solubilized membranes extracted from aerobically grown cells by a combination of anion-exchange and size-exclusion chromatography. Both OGP and Thesit (when used at a protein-to-detergent ratio of ~1:1) were successful for solubilization and purification of the selenate reductase, but it was found that the enzyme purified using OGP was less stable and degraded rapidly over several hours. The effects of both temperature and oxygen sensitivity were also assessed prior to purification. A Source 30Q column was equilibrated with 50 mM Tris-HCl, 2% (wt/vol) Thesit, pH 8.6, using a constant flow rate of 1 ml/min. Thesit-solubilized membrane fractions (10 ml) were filtered through a 0.2-μm filter and loaded onto the column at 1 ml/min, and the flowthrough was collected. The column was washed with 100% buffer A at 1 ml/min until all unbound proteins were removed. The bound proteins were eluted using a step gradient of 20% 50 mM Tris-HCl, 1 M NaCl, 2% (wt/vol) Thesit, pH 8.6, and the proteins were collected in 0.5-ml fractions. Again, a large protein peak was eluted at 200 mM NaCl, with the selenate reductase activity located to the right of the major peak. The fractions with the highest activities were pooled and loaded onto a Superdex 200 prep-grade column (60 ml; Amersham Biosciences) pre-equilibrated with 50 mM Tris-HCl, 100 mM NaCl, 2% (wt/vol) Thesit, pH 8.6, at 1 ml/min. The sample was injected at 1 ml/min, and the eluted protein was collected as 1-ml fractions. These fractions were analyzed for selenate, nitrate, and chlorate reductase activities and were analyzed by sodium dodecyl sulfate-polyacrylamide gel electrophoresis (SDS-PAGE). In order to determine the molecular weights of the active peaks, a molecular weight calibration kit (Amersham Biosciences) was utilized according to the manufacturer's instructions.

Spectrophotometric enzyme activity assays. Reductase activities of purified proteins and cell fractions were measured in a cuvette (3 ml) at 20°C by following the oxidation of reduced methyl viologen spectrophotometrically at 600 nm (6), coupled to the reduction of substrates or potential substrates. These included sodium selenate, sodium selenite, potassium nitrate, potassium nitrite, potassium chlorate, potassium chlorite, sodium perchlorate, potassium bromate, potassium arsenate, potassium sulfate, potassium thiosulfate, dimethyl sulfoxide (DMSO), and trimethylamine-*N*-oxide (TMAO). Substrates were assayed at a range of concentrations. Activities, where detected, were calculated from the initial rates by using an extinction coefficient of 13,700 M^{-1} cm^{-1} for the methyl viologen radical. Values for K_m and V_{max} cited in the text and tables are the mean values ($n = 3$) calculated using nonlinear regression analysis in Grafit v3.0 (Erithacus Software).

In order to assay multiple fractions eluted from the anion-exchange and size-exclusion columns, a microtiter plate assay was developed. Incubation buffer (50 mM potassium phosphate, pH 7.2, 1 mM methyl viologen) was placed in a rubber septum-sealed bottle, purged with O_2-free nitrogen gas for 20 min, and equilibrated to 30°C. Sodium dithionite (0.5 M) was prepared, purged with nitrogen, and equilibrated to 30°C. Stock substrate solutions of sodium selenate (1 M), potassium nitrate (1 M), potassium chlorate (0.5 M), potassium bromate (0.5 M), sodium thiosulfate (1 M), and sodium perchlorate (0.5 M) were prepared in sterile water in septum-sealed bottles and purged with nitrogen for 20 min. Fractions eluted from the size-exclusion column (50 μl) and incubation buffer (141 μl) were added to the wells of a 96-well flat-bottomed microtiter plate. Blank wells contained incubation buffer (191 μl) only. Sodium dithionite (3 μl) was added to each well and mixed. To initiate the reaction, substrates were added at the following final concentrations: selenate, 30 mM; thiosulfate, 30 mM; perchlorate, 30 mM; TMAO, 30 mM; DMSO, 30 mM; nitrate, 15 mM; chlorate, 15 mM; and bromate, 30 mM. Immediately following the addition of substrate, the absorbance at 600 nm was measured using a UV/Vis plate reader and monitored until no further absorbance changes were detected.

Polyacrylamide gel electrophoresis and activity/heme staining. SDS-PAGE was done using gels with a 12% linear gradient of acrylamide and a discontinuous buffer system. Proteins were also separated using nondenaturing PAGE (6% Tris-glycine gels), and gels were stained with dithionite-reduced methyl viologen (5 mM) under anaerobic conditions, using a small anaerobic chamber built in-house and purged with O_2-free nitrogen for 30 min. Protein bands with selenate or nitrate reductase activity were identified by the addition of either selenate or nitrate for 15 min and observed as clear bands due to the substrate-dependent reoxidation of reduced methyl viologen, changing the color from dark blue to colorless. Staining for heme-linked peroxidase activity was performed as described previously (29).

Protein sequencing. Protein subunits identified for N-terminal sequencing analysis were blotted from SDS-PAGE gels onto polyvinylidene difluoride membranes. N-terminal amino acid sequence determination was attempted by the molecular biology facility at the University of Newcastle.

Spectroscopy. The oxidized and dithionite-reduced electron absorption spectra of the purified selenate reductase were recorded using a Varian Cary 4E UV/visible spectrophotometer. The electron paramagnetic resonance (EPR) spectrum of the Mo(V) species of nitrate reductase (NarG) was measured at 70 K by using a Bruker EMX spectrometer (X-band at 9.38 GHz) equipped with an ER4112HV liquid-helium-flow cryostat system. Iron and molybdenum contents were determined by using a Thermo electron solar atomic absorption spectrophotometer and comparing the results to standard calibration curves prepared from Fe and Mo standards (Fisher Scientific).

DNA sequencing. An internal portion of the *narG* homolog was amplified by PCR from the *E. cloacae* SLD1a-1 genome. Conditions were maintained as described by Gregory et al. (11) by use of Thermostart master mix (ABgene) and degenerate primers designed from a composite of nitrate reductase sequences (T37 and T39) (11). The PCR fragment (~1.3 kb) was ligated to the pGEMT vector (Promega), transformed into competent *E. coli* JM109 cells, and cultivated. The plasmid was extracted using the Fastplasmid method (Eppendorf), and then a lyophilized sample was supplied to MWG-Biotech for sequencing using primers for the T7 and SP6 promoter regions.

Nucleotide sequence accession number. The *E. cloacae* SLD1a-1 *narG* DNA sequence has been deposited with GenBank under accession number DQ355973.

RESULTS

The membrane-bound nitrate reductase from *E. cloacae* SLD1a-1 is typical of the NAR family but does not reduce selenate. Previous studies of whole cells of *E. cloacae* SLD1a-1 have suggested that the membrane-bound nitrate reductase is not involved in the process of selenate reduction (31). To test this hypothesis, the nitrate reductase was purified and assayed for selenate reductase activity in vitro. Purification of the nitrate reductase from solubilized membranes was followed using SDS-PAGE, nondenaturing PAGE, and activity assays. The nitrate reductase enzyme was purified to homogeneity by using two sequential anion-exchange columns. SDS-PAGE of the purified nitrate reductase showed two peptides resolved at molecular masses of ~140 kDa and ~58 kDa (Fig. 1A), and by analogy to membrane-bound nitrate reductases from other organisms, these have been designated the α and β subunits, respectively. The third, γ subunit that is present in other prototype NAR enzymes (NarI component) was not detectable by SDS-PAGE and may have been lost during the purification procedure. Furthermore, attempts to detect the *b*-type cytochrome moiety by electronic absorption spectroscopy were unsuccessful. The sizes of the α and β subunits are comparable to those of the NarG and NarH subunits in other enteric bacteria,

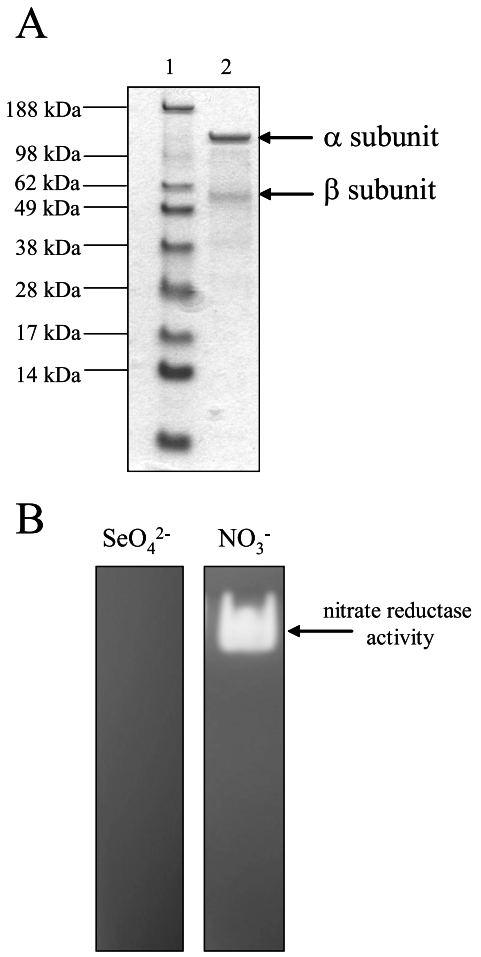

FIG. 1. Purified membrane-bound nitrate reductase. (A) SDS-PAGE gel stained with Simply Blue Safestain (Invitrogen). Lane 1, molecular size marker; lane 2, purified nitrate reductase resolved into α and β subunits. (B) Native PAGE gel with purified nitrate reductase stained for activity using reduced methyl viologen (5 mM) as the electron donor and developed by the addition of nitrate (10 mM) or selenate (50 mM). Nitrate reductase activity is indicated.

for example, *E. coli* NarG is ~140 kDa and NarH is ~58 kDa (4, 14). Using degenerate primers (T37 and T39) derived from multiple alignments of NarG sequences (11), a 1,393-bp fragment of the *E. cloacae* SLD1a-1 NarG gene was PCR amplified and sequenced. The translated amino acid sequence showed ~93% identity to NarG from *E. coli*, with all redox cofactor ligands being conserved. The purified α/β complex displayed nitrate reductase activity, with the following catalytic constants: $K_m(NO_3^-)$, 0.24 mM; and V_{max}, 1.0 μmol NO_3^- min^{-1} mg^{-1}. It also displayed chlorate reductase activity, with the following catalytic constants: $K_m(ClO_3^-)$, 0.52 mM; and V_{max}, 1.5 μmol ClO_3^- min^{-1} mg^{-1}. Metal analysis of the α/β complex gave total metal contents of 18 ± 0.8 mol Fe per mol of enzyme and 0.8 ± 0.06 mol Mo per mol of enzyme, consistent with the α and β subunits coordinating the five iron-sulfur clusters and the Mo cofactor that are present in the *E. coli* homologue (4, 14). Further analysis of the Mo center by EPR spectroscopy gave Mo(V) signals typical of those observed for the low-pH form of NarG from *E. coli* (data not shown). The purified α/β complex was resolved as a single band on native PAGE gels and produced a strong clear band when stained for nitrate reductase activity (Fig. 1B). Attempts to detect any selenate reductase activity were unsuccessful. Cuvette-based spectrophotometric assays in the presence of increasing selenate concentrations of up to 200 mM did not detect any enzyme-dependent reoxidation of either methyl or benzyl viologen. Furthermore, native PAGE gels stained with reduced methyl viologen and submerged in selenate (100 mM) failed to reveal clear bands indicative of selenate reductase activity (Fig. 1B). In order to determine whether selenate was actually binding to the active site of the enzyme, nitrate reductase rates were measured in the presence of increasing selenate concentrations (0 to 200 mM). With the nitrate concentration fixed at 1 mM, the rate of nitrate reduction remained constant with increasing selenate concentrations. No selenate-dependent inhibition was observed. Similarly, with the nitrate concentration fixed well below the K_m for nitrate, at 0.1 mM, again there was no observed inhibition of the nitrate reductase activity. These data strongly suggest that the selenate reduction observed in whole cells is not catalyzed by the respiratory nitrate reductase and that another membrane-bound enzyme must be utilized instead.

Purification and subunit composition of membrane-bound selenate reductase from *E. cloacae* SLD1a-1. Having established that the membrane-bound nitrate reductase was not involved in the selenate reducing pathway, isolation of the selenate reductase became the major objective. *E. cloacae* SLD1a-1 grown aerobically on LB medium in the presence of selenate (10 mM) readily reduces selenate and selenite to elemental selenium, forming a brick-red precipitate. The production of precipitated selenium was enhanced by the presence of additional sodium molybdate in the culture medium (32). We have also demonstrated previously that cultures grown in the presence of sodium tungstate (10 mM) inhibit the selenate reductive pathway, suggesting the involvement of a molybdoenzyme (32). In attempts to purify the enzyme responsible for selenate reduction, cultures were grown in the presence of 1 mM sodium molybdate, and selenate reductase activity was monitored in growing cultures in order to obtain maximum reductase yields. Selenate reductase activity was typically maximal in cells grown for between 4 and 9 h (Fig. 2), after which the activity decreased significantly. Increasing the molybdate concentration from 1 mM to 20 mM and/or varying the temperature had no or little effect on the level of selenate reductase activity. Selenate reductase activity was located solely in the membrane fraction, and the active enzyme (~2.2 μmol SeO_4^{2-} min^{-1} ml^{-1}) was extracted successfully from membranes by using either OGP or Thesit (2.0 to 2.5% [wt/vol]) detergent. The enzyme extracted using OGP, however, was labile, and its activity was readily lost after it was stored for a few hours at either 4 or −20°C. The enzyme extracted with Thesit remained active for 24 h when stored at 4°C and retained >50% activity after being frozen at −20°C for prolonged periods. Given the inherent instability of the selenate reductase complex once extracted from the membrane, the

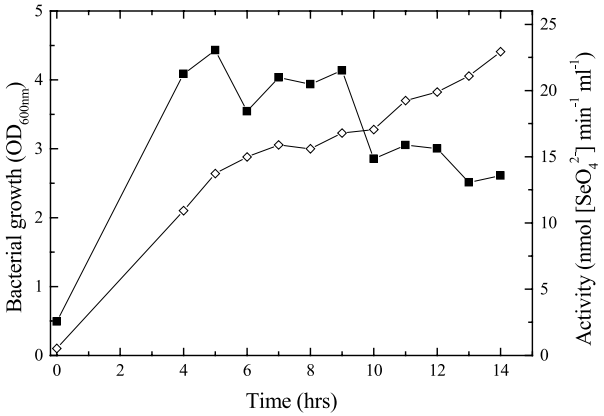

FIG. 2. Growth curve and selenate reductase activity profile for *E. cloacae* SLD1a-1. Cells were cultured aerobically in the presence of 1 mM sodium molybdate, and growth was monitored by the optical density at 600 nm (OD_{600}) (◇). Selenate reductase activity (■) was measured using methyl viologen as the electron donor. The data presented are typical of the results obtained for three independent experiments.

TABLE 1. Purification summary for the membrane-bound selenate reductase from *E. cloacae* SLD1a-1

Purification step or sample	Total vol (ml)	Total activity (nmol SeO_4^{2-} min^{-1})[b]	Total protein (mg)	Sp act (nmol SeO_4^{2-} min^{-1} mg^{-1})[b]	Purification (fold)
Membrane fraction	23.0	28,000.0	513.3	54.0	1.0
Solubilized membranes	7.5	7,000.0	151.6	47.0	0.9
Source Q30 chromatography (active peak)	3.0	1,300.0	19.1	68.0	1.3
Superdex 200 chromatography[a]	4.0	200.0	0.4	500.0	9.3

[a] Selenate reductase holoenzyme (~600 kDa).
[b] Variation in activities was within 10% of the mean values shown.

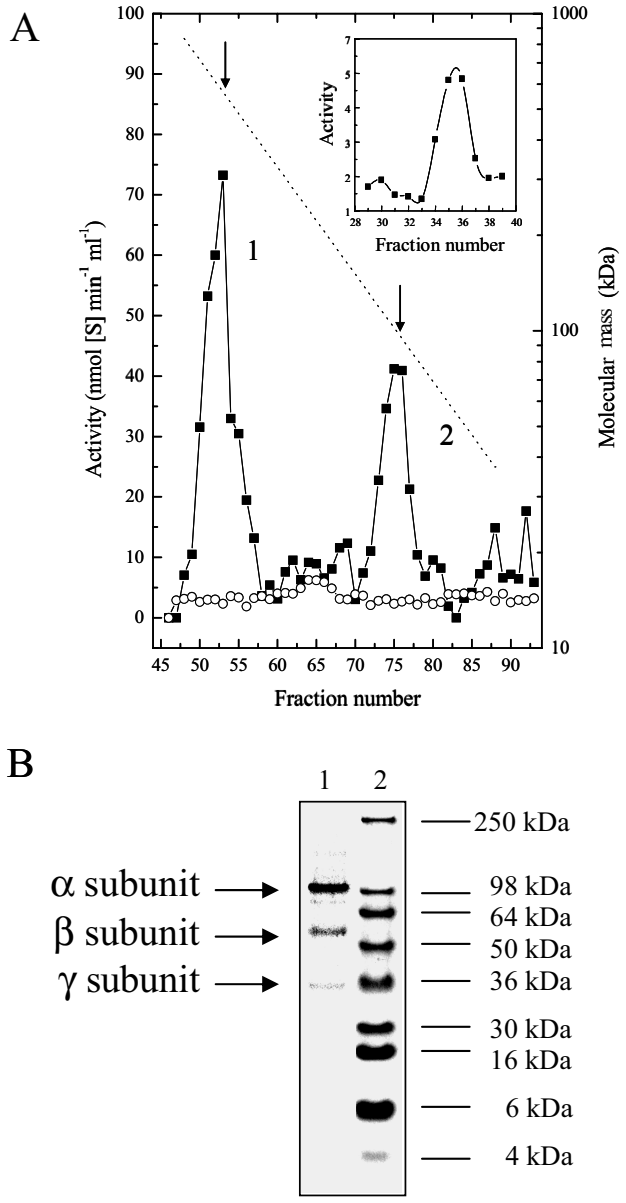

FIG. 3. Purification of membrane-bound selenate reductase. (A) Reductase activities in fractions eluted from a Superdex 200 column, assayed with selenate (■) and nitrate (○) as substrates by the microtiter plate method. The column was calibrated using thyroglobin (655 kDa), ferritin (398 kDa), catalase (226 kDa), and cytochrome *c* (12 kDa) as molecular size markers (dotted line). Fraction numbers represent the elution volume in milliliters. Peaks with selenate reductase activity, labeled 1 and 2, were resolved at molecular masses of ~600 kDa and ~100 kDa, respectively, as indicated by the arrows. The data presented are typical of the results obtained from five independent batches of protein. The inset shows the activity profile for fractions eluted during Source 30Q anion-exchange chromatography. (B) SDS-PAGE analysis of pure selenate reductase (lane 1). Lane 2, molecular size marker.

present purification protocol and characterization have been developed with over 50 batches of solubilized membranes, and the purification process is now routinely completed within a 16-h time frame.

The progressive purification of the selenate reductase from solubilized membranes was again monitored by SDS-PAGE, nondenaturing PAGE, and activity assays. The selenate reductase enzyme was purified to homogeneity using a combination of anion-exchange and size-exclusion chromatography. The overall purification scheme and yields from a typical purification preparation are detailed in Table 1. The peak fraction with maximum selenate reductase activity was eluted from the Source 30Q column at ~200 mM NaCl (Fig. 3A, inset). No nitrate reductase activity was detected in this fraction, but activity was detected with chlorate as a substrate, resolving into two distinct activity peaks. Fractions displaying selenate reductase activities of >2.5 μmol SeO_4^{2-} min^{-1} ml^{-1} were pooled and loaded onto a Superdex 200 size-exclusion column. In order to track eluted active fractions, a microtiter plate, methyl viologen-based assay was developed. This allowed for the rapid identification of active fractions and permitted a range of substrates to be tested simultaneously. The elution profile from the size-exclusion column is shown in Fig. 3A. Fractions F46-96 were assayed for both selenate- and nitrate-dependent reoxidation of reduced methyl viologen in the microtiter plate assay. Two peak fractions were detected, with maximum selenate reductase activities of 75 nmol SeO_4^{2-} min^{-1} ml^{-1} and 40 nmol SeO_4^{2-} min^{-1} ml^{-1}. These active fractions corresponded to complexes with molecular masses of ~600 and ~100 kDa, respectively. No reductase activity was detected in either peak when nitrate, sulfate, perchlorate, or thiosulfate was used as the substrate. Selenate reductase and nitrate reductase activities, when measurable in the same sample, did not coelute from any of the columns. Analysis of the ~600-kDa peak fraction (F53) by SDS-PAGE resolved the presence of three distinct peptides, migrating to positions corresponding to molecular masses of ~100, ~55, and ~36 kDa (Fig. 3B). SDS-PAGE analysis of the fraction corresponding to the ~100-kDa activity peak (F73-76) revealed the presence of a number of smaller peptides of between 40 and 60 kDa and a distinct band at ~100 kDa (not shown). It is considered unlikely that the ~100-kDa protein is a distinct second selenate reductase since only one activity band was observed in solubilized membrane fractions resolved by nondenaturing PAGE (Fig. 4A, lane 2). We speculate that the ~100-kDa protein represents the active subunit dissociated from the holocomplex. In order to confirm the overall enzyme subunit composition, membranes displaying high selenate reductase activities were solubilized (2% [wt/vol] Thesit) and analyzed by nondenaturing PAGE, and activity was stained to reveal the location of the selenate reductase (Fig. 4A). The active band was extracted from the gel, and the protein was electroeluted and subsequently analyzed by SDS-PAGE. Peptides with molecular masses of ~100 kDa, ~55 kDa, and ~36 kDa were again resolved (data not shown). The combined data from these studies strongly suggest that the selenate reductase complex comprises only three subunits. Given that the holocomplex has an observed molecular mass of ~600 kDa, we suggest that when the complex is solubilized in Thesit detergent, the overall subunit arrangement forms a trimer of heterotrimers ($\alpha_3\beta_3\gamma_3$), giving a calculated mass of 573 kDa. This subunit arrangement resembles that of formate dehydrogenase N from *E. coli*, whose crystal structure also displays an $\alpha_3\beta_3\gamma_3$ subunit composition, with an overall molecular mass of 510 kDa (15).

The three distinct peptides resolved by SDS-PAGE from the

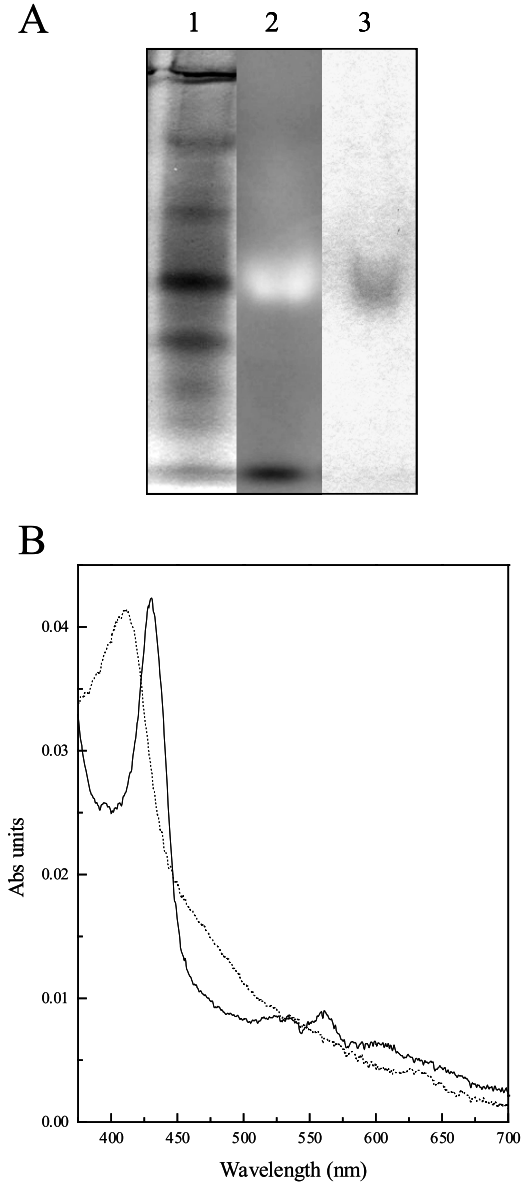

FIG. 4. Subunit composition and heme analysis of the membrane-bound selenate reductase. (A) Native PAGE gel with solubilized membranes stained for the following: lane 1, total protein; lane 2, selenate reductase activity; and lane 3, heme Fe. (B) Electronic absorption spectra of membrane-bound selenate reductase from *E. cloacae* SLD1a-1. The purified enzyme was used at a protein concentration of 86 μg/ml. Spectra for the air-oxidized enzyme (dotted line) and sodium dithionite-reduced enzyme (solid line) are shown.

600-kDa active peak were blotted and extracted for N-terminal sequence analysis. N-terminal sequencing of the peptides after separation by SDS-PAGE was unsuccessful, however, suggesting N-terminal blocking of all subunits. Metal analysis of the ~600-kDa complex gave total metal contents of 18.4 ± 0.8 mol Fe per mol of enzyme and 0.6 ± 0.2 mol Mo per mol of enzyme, consistent with the coordination of a Mo cofactor and a number of iron-containing centers. Evidence for the presence of a heme-containing subunit in the selenate reductase complex was demonstrated by heme stain analysis of nondenatured membrane fractions (Fig. 4A). The heme-stained gel (lane 3) clearly show a protein at the corresponding position to that detected for selenate reductase activity. The presence of covalently attached *c*-type cytochromes was not detected for the denatured protein in SDS gels. The purified oxidized selenate reductase complex exhibited an electronic absorbance spectrum with a Soret maximum at 411 nm. Broad absorption bands are also visible from 420 to 500 nm and 600 to 650 nm, possibly arising from oxidized [Fe-S] clusters and Mo(VI), respectively. Upon reduction with sodium dithionite, these features are lost and replaced with absorbance maxima at 428 nm, ~528 nm, and ~556 nm, which are characteristic of reduced *b*-type cytochromes (Fig. 4B), and a broad feature at 575 to 625 nm, possibly from Mo(IV). The cytochrome content was determined to be 0.9 ± 0.14 mol of heme per mol of enzyme based upon the extinction coefficient of cytochrome *b* ($\varepsilon_{556\text{-}540\ nm}$ = 24 mM^{-1} cm^{-1}) and the predicted molecular mass (600 kDa) of the selenate reductase complex. The involvement of cytochromes in selenate reduction was demonstrated by monitoring the selenate-dependent reoxidation of the reduced cytochromes at 556 nm. Additional analysis of the metal centers of selenate reductase by EPR spectroscopy at this stage was not possible due to the low concentration of pure sample. These data suggest that the selenate reductase complex comprises three subunits with an overall molecular mass of ~600 kDa and includes an ~100-kDa molybdenum-binding active α subunit that readily dissociates from the iron-sulfur- and heme-containing holocomplex during purification. The functional involvement of cytochromes and the presence of nonheme iron suggest that the γ and β subunits form a conventional electron transfer chain, mediating the transfer of electrons from the Q pool to the selenate reductase active site, and as such, the selenate reductase resembles other well-characterized membrane-bound molybdo-enzymes.

Specificity for selenate and nitrate. Kinetic analysis (Table 2) of the purified selenate reductase holocomplex (~600 kDa), using reduced methyl viologen as the electron donor, revealed that in addition to reducing selenate [K_m(SeO_4^{2-}), 2.1 mM; V_{max}, 0.5 μmol SeO_4^{2-} min^{-1} mg^{-1}], the complex also used chlorate [K_m(ClO_3^-), 3.0 mM; V_{max}, 0.035 μmol ClO_3^- min^{-1} mg^{-1}] as a substrate. Based upon the native molecular mass of 600 kDa, the membrane-bound selenate reductase reduces sel-

TABLE 2. Kinetic properties of membrane-bound nitrate and selenate reductases

Pure enzyme	Kinetic constant[a]			
	Nitrate (NO_3^-)		Selenate (SeO_4^{2-})	
	K_m (mM)	V_{max} (U mg^{-1})[b]	K_m (mM)	V_{max} (U mg^{-1})[b]
Nitrate reductase	0.24	1.0		ND
Selenate reductase				
~600-kDa holoenzyme		ND	2.1	0.50
~100-kDa active α subunit		ND	5.5	0.34

[a] Kinetic constants were measured by using methyl viologen as the electron donor. Variation was within 10% of the mean values shown (n = 3).

[b] Units are defined in μmol (S) min^{-1}. ND, activity not detected (<0.005 μmol [S] min^{-1} mg^{-1}).

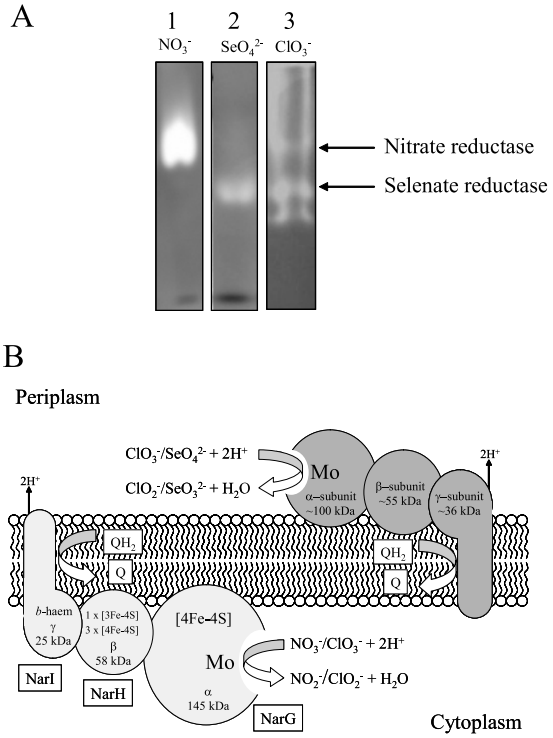

FIG. 5. Resolution of selenate and nitrate reductases in membrane fractions of *E. cloacae* SLD1a-1, using nitrate, selenate, and chlorate as substrates. (A) Native PAGE gels with solubilized membranes. Gel 1, solubilized membranes from cells grown anaerobically using nitrate as the sole electron acceptor and stained for nitrate reductase activity; gel 2, solubilized membranes from cells grown aerobically and stained for selenate reductase activity; gel 3, solubilized membranes from cells grown aerobically and stained for chlorate reductase activity. The distinct reductases are indicated. (B) Model showing subunit composition of the membrane-bound nitrate and selenate reductases from *E. cloacae* SLD1a-1.

enate at a calculated turnover rate (k_{cat}) of 5.0 s^{-1} (k_{cat}/K_m = ~2.4 × 10^3 s^{-1} M^{-1}) and chlorate at a turnover rate (k_{cat}) of 0.35 s^{-1} (k_{cat}/K_m = ~117 s^{-1} M^{-1}). A low level of activity was also detected with bromate as a substrate (catalytic constants were not determined). The purified enzyme displayed no reductase activity when nitrate, sulfate, perchlorate, DMSO, TMAO, or thiosulfate was tested as the substrate. The selenate reductase activity of the ~100-kDa fraction was also examined, and the observed kinetic constants were as follows: $K_m(SeO_4^{2-})$, 5.5 mM; and V_{max}, 0.34 μmol SeO_4^{2-} min^{-1} mg^{-1} (Table 2).

Simultaneous resolution of distinct nitrate and selenate reductases in membrane fractions. In order to simultaneously demonstrate the presence of the distinct nitrate and selenate reductases in membrane fractions from *E. cloacae* SLD1a-1, solubilized proteins were separated by native PAGE, and activity was stained using nitrate, selenate, and chlorate as substrates (Fig. 5A). Nitrate reductase activity was detected predominantly in membranes from cells grown anaerobically with nitrate as the sole electron acceptor. A low level of nitrate reductase activity was also detectable in membranes from cells grown under aerobic conditions. Selenate reductase activity was detected predominantly in membranes from aerobically grown cells but could not be detected by native PAGE in membranes from cells grown anaerobically in the presence of nitrate. Membrane proteins stained for chlorate reductase activity clearly showed the activities due to both the nitrate and selenate reductases and unequivocally resolved the presence of the two enzymes in the total membrane fraction. A third chlorate activity band was also observed from a protein that migrated further than the nitrate and selenate reductases. This protein displayed no activity towards nitrate or selenate and may correspond to a chlorate-specific reductase.

DISCUSSION

The present work describes the purification and characterization of distinct selenate and nitrate reductases from the cytoplasmic membrane of *E. cloacae* SLD1a-1. The nitrate reductase is typical of the NAR family and purifies as a NarGH homodimer. The enzyme displays reductase activity towards both nitrate and chlorate but shows no detectable selenate reductase activity. This is in contrast to the low level of selenate reductase activity that has been reported previously for other members of the NAR family, as exemplified by the NAR proteins from *E. coli* (1) and *P. denitrificans* (25). The observation that selenate does not compete with nitrate for the active site of the nitrate reductase may prove advantageous for cell survival in selenate-rich environments. By selectively reducing nitrate only under anaerobic conditions, *E. cloacae* SLD1a-1 may avoid the inevitable generation of toxic levels of selenite that would accumulate within the cell when growing under selenate-rich, oxygen-limited conditions.

The membrane-bound selenate reductase is the first of its type to be purified to homogeneity. The molybdo-enzyme complex comprises three subunits, with molecular masses of ~100 kDa, ~55 kDa, and ~36 kDa (Fig. 5B). The enzyme displays no apparent nitrate reductase activity but readily reduces the substrates chlorate and bromate, although with lower affinities than that for selenate. The enzyme shows a number of features similar to those of the well-characterized periplasmic SER from *T. selenatis* (17, 26). Notably, both are molybdo-enzymes, their catalytic α subunits are of similar sizes (SerA is ~96 kDa), both are unable to reduce nitrate, both contain *b*-type cytochromes, and both have active sites located in the periplasm. Furthermore, although it was previously not reported, both SER and the membrane-bound selenate reductase from *E. cloacae* SLD1a-1 readily reduce chlorate. The obvious difference between SER and the membrane-bound enzyme reported in this study is that SER is freely soluble in the periplasm and not anchored to the cytoplasmic membrane. The affinities for selenate of the two enzymes are also markedly different. The observed K_m for selenate of SER is ~16 μM, in contrast to the low affinity (K_m, ~2 mM) of the membrane-bound enzyme. However, the observed K_m for the membrane-bound selenate reductase may be misleadingly high owing to the use of a nonphysiological electron donor. It has been reported that the K_m for nitrate of NAR from *P. denitrificans* is ~20-fold lower when determined using duroquinol rather than methyl viologen (6).

The membrane-bound selenate reductase from *E. cloacae* SLD1a-1, unlike other similar molybdo-enzymes, including SerABC from *T. selenatis*, cannot support anaerobic growth on

nonfermentable carbon substrates and seems to have a role only in selenate detoxification. The combination of low substrate affinity and the fact that QH_2-selenate electron transfer is not electrogenic may well suit its detoxification role, since the process will only function at elevated/toxic selenate concentrations and will not be subjected to negative thermodynamic feedback via the proton motive force generated through aerobic respiration. The observation that the membrane-bound selenate reductase is not up regulated under anaerobic growth conditions or induced by the presence of a substrate in the growth medium further supports its function in detoxification rather than respiration and highlights that it has a very different mechanism of transcriptional control than both NAR and SER.

Finally, factors that control the substrate selectivity of the oxyanion reductases remain to be established. Modeling the SerA component from the periplasmic selenate reductase on the crystal structure of the respiratory nitrate reductase from *E. coli* identified a number of highly conserved residues within NarG, surrounding the active site and the proposed substrate entry channel, that may enhance selectivity towards trigonal planar (NO_3^-) rather than tetrahedral (SeO_4^{2-}) substrates (8). Furthermore, the difference in charge between selenate and nitrate may also be a means by which the oxyanions are discriminated. Attempts to locate and sequence the genes encoding the individual subunits of the membrane-bound selenate reductase are currently in progress and should provide further insight into the regulation, mechanism of substrate selection, and molecular structure of this novel enzyme.

ACKNOWLEDGMENTS

This work was supported by BBSRC research grants (13/P17219 and BBS/B/10110) to C.S.B. and D.J.R.

We thank Joe Gray (Molecular Biology Facility, University of Newcastle) for help with peptide sequencing and Duncan Harvey (University of Newcastle) for help with the metal analysis. We also thank James Allen (University of Oxford) and Joanne Santini (University College London) for useful discussions.

REFERENCES

1. **Avazeri, C., R. J. Turner, J. Pommier, J. H. Weiner, G. Giordano, and A. Verméglio.** 1997. Tellurite reductase activity of the nitrate reductase is responsible for the basal resistance of *Escherichia coli* to tellurite. Microbiology **143:**1181–1189.
2. **Bébien, M., J. Kirsch, V. Méjean, and A. Verméglio.** 2002. Involvement of a putative molybdenum enzyme in the reduction of selenate by *Escherichia coli*. Microbiology **148:**3865–3872.
3. **Bender, K. S., C. Shang, R. Chakraborty, S. M. Belchik, J. D. Coates, and L. A. Achenbach.** 2005. Identification, characterization, and classification of genes encoding perchlorate reductase. J. Bacteriol. **187:**5090–5096.
4. **Bertero, M. G., R. A. Rothery, M. Palak, C. Hou, D. Lim, F. Blasco, J. H. Weiner, and N. C. Strynadka.** 2003. Insights into the respiratory electron transfer pathway from the structure of nitrate reductase A. Nat. Struct. Biol. **10:**681–687.
5. **Butler, C. S., J. M. Charnock, B. Bennett, H. J. Sears, A. J. Reilly, S. J. Ferguson, C. Garner, D. J. Lowe, A. J. Thomson, B. C. Berks, and D. J. Richardson.** 1999. Models for molybdenum co-ordination during the catalytic cycle of periplasmic nitrate reductase from *Paracoccus denitrificans* derived from EPR and EXAFS spectroscopy. Biochemistry **38:**9000–9012.
6. **Craske, A., and S. J. Ferguson.** 1986. The respiratory nitrate reductase from *Paracoccus denitrificans*. Molecular characterisation and kinetic properties. Eur. J. Biochem. **158:**429–436.
7. **DeMoll-Decker, H., and J. M. Macy.** 1993. The periplasmic nitrite reductase of *Thauera selenatis* may catalyse the reduction of selenite to elemental selenium. Arch. Microbiol. **160:**241–247.
8. **Dridge, E. J., D. J. Richardson, R. J. Lewis, and C. S. Butler.** 2006. Developing structure-based models to predict substrate specificity of D-group (type II) molybdenum enzymes: application to a molybdo-enzyme of unknown function from *Archaeoglobus fulgidus*. Biochem. Soc. Trans. **34:**118–121.
9. **Dungan, R. S., and W. T. Frankenberger.** 2001. Biotransformation of selenium by *Enterobacter cloacae* SLD1a-1: formation of dimethylselenide. Biogeochemistry **55:**73–86.
10. **Focht, D. D.** 1994. Microbiological procedures for biodegradation research, p. 407–426. *In* Methods of soil analysis, part 2. Microbiological and biochemical properties. Soil Science Society of America, Madison, Wis.
11. **Gregory, L. G., P. L. Bond, D. J. Richardson, and S. Spiro.** 2003. Characterization of a nitrate-respiring bacterial community using the nitrate reductase gene (narG) as a functional marker. Microbiology **149:**229–237.
12. **Haygarth, P. M.** 1994. Global importance and global cycling of selenium, p. 1–28. *In* W. T. Frankenberger, Jr., and S. Benson (ed.), Selenium in the environment. Marcel Dekker, New York, N.Y.
13. **Johnson, H. A., D. A. Pelletier, and A. M. Spormann.** 2001. Isolation and characterization of anaerobic ethylbenzene dehydrogenase, a novel Mo-Fe-S enzyme. J. Bacteriol. **183:**4536–4542.
14. **Jormakka, M., D. Richardson, B. Byrne, and S. Iwata.** 2004. Architecture of NarGH reveals a structural classification of Mo-*bis*MGD enzymes. Structure **12:**95–104.
15. **Jormakka, M., S. Törnroth, B. Byrne, and S. Iwata.** 2002. Molecular basis of proton motive force generation: structure of formate dehydrogenase-N. Science **295:**1863–1868.
16. **Kessi, J., and K. W. Hanselmann.** 2004. Similarities between the abiotic reduction of selenite with glutathione and the dissimilatory reaction mediated by *Rhodospirillum rubrum* and *Escherichia coli*. J. Biol. Chem. **279:**50662–50669.
17. **Krafft, T., A. Bowen, F. Theis, and J. M. Macy.** 2000. Cloning and sequencing of the genes encoding the periplasmic-cytochrome *b*-containing selenate reductase from *Thauera selenatis*. DNA Seq. **10:**365–377.
18. **Losi, M. E., and W. T. Frankenberger.** 1997. Reduction of selenium oxyanions by *Enterobacter cloacae* SLD1a-1: isolation and growth of the bacterium and its expulsion of selenium particles. Appl. Environ. Microbiol. **63:**3079–3084.
19. **Macy, J. M., S. Rech, G. Auling, M. Dorsch, E. Stackenbrandt, and L. I. Sly.** 1993. *Thauera selenatis* gen. nov., sp. nov., a member of the beta-subclass of proteobacteria with a novel type of anaerobic respiration. Int. J. Syst. Bacteriol. **43:**135–142.
20. **Maher, M. J., J. Santini, I. J. Pickering, R. C. Prince, J. M. Macy, and G. N. George.** 2004. X-ray absorption spectroscopy of selenate reductase. Inorg. Chem. **43:**402–404.
21. **McDevitt, C. A., P. Hugenholtz, G. R. Hanson, and A. G. McEwan.** 2002. Molecular analysis of dimethyl sulphide dehydrogenase from *Rhodovulum sulfidophilum*: its place in the dimethyl sulphoxide reductase family of microbial molybdopterin-containing enzymes. Mol. Microbiol. **44:**1575–1587.
22. **Oremland, R. S., N. A. Steinberg, T. S. Presser, and L. G. Miller.** 1991. In situ bacterial selenate reduction in the agricultural drainage systems of western Nevada. Appl. Environ. Microbiol. **57:**615–617.
23. **Oremland, R. S., J. Switzer Blum, A. Burns Bindi, P. R. Dowdle, M. Herbel, and J. F. Stolz.** 1999. Simultaneous reduction of nitrate and selenate by cell suspensions of selenium-respiring bacteria. Appl. Environ. Microbiol. **65:**4385–4392.
24. **Rayman, M.** 2002. Se brought to Earth, p. 28–31. *In* Chemistry in Britain.
25. **Sabaty, M., C. Avazeri, D. Pignol, and A. Verméglio.** 2001. Characterization of the reduction of selenate and tellurite by nitrate reductases. Appl. Environ. Microbiol. **67:**5122–5126.
26. **Schröder, I., S. Rech, T. Krafft, and J. M. Macy.** 1997. Purification and characterization of the selenate reductase from *Thauera selenatis*. J. Biol. Chem. **272:**23765–23768.
27. **Stadtman, T. C.** 1996. Selenocysteine. Annu. Rev. Biochem. **65:**83–100.
28. **Stolz, J. F., and R. S. Oremland.** 1999. Bacterial respiration of arsenic and selenium. FEMS Microbiol. Rev. **23:**615–627.
29. **Thomas, P. E., D. Ryan, and W. Levin.** 1976. An improved staining procedure for the detection of the peroxidase activity of cytochrome P-450 on sodium dodecyl sulfate polyacrylamide gels. Anal. Biochem. **75:**168–176.
30. **Thorell, H. D., K. Stenklo, J. Karlsson, and T. Nilsson.** 2003. A gene cluster for chlorate metabolism in *Ideonella dechloratans*. Appl. Environ. Microbiol. **69:**5585–5592.
31. **Watts, C. A., H. Ridley, E. J. Dridge, J. T. Leaver, A. J. Reilly, D. J. Richardson, and C. S. Butler.** 2005. Microbial reduction of selenate and nitrate: common themes and variations. Biochem. Soc. Trans. **33:**173–175.
32. **Watts, C. A., H. Ridley, K. L. Condie, J. T. Leaver, D. J. Richardson, and C. S. Butler.** 2003. Selenate reduction by *Enterobacter cloacae* SLD1a-1 is catalysed by a molybdenum-dependent membrane bound enzyme that is distinct from the nitrate reductase. FEMS Microbiol. Lett. **228:**273–279.